sciendo

POLISH MARITIME RESEARCH 4 (116) 2022 Vol. 29; pp. 12-25
10.2478/pomr-2022-0040

SIMULATION OF TURNING MANOEUVRE OF PLANING CRAFT TAKING INTO ACCOUNT THE RUNNING ATTITUDE CHANGE IN A SIMPLIFIED MANNER

Kazem Sadati
Hamid Zeraatgar *
Aliasghar Moghaddas
Amirkabir University of Technology, Department of Maritime Engineering, Tehran, Islamic Republic of Iran

* Corresponding author: *hamidz@aut.ac.ir (H. Zeraatgar)*

ABSTRACT

The modelling and simulation of planing craft manoeuvres requires coupled six degrees of freedom (6 DOF) motion equations. A coupled 6 DOF motion equation needs hundreds of manoeuvring hydrodynamic coefficients (MHCs) that are mostly determined using the planar motion mechanism (PMM) test. The number of test runs is too high, unless a kind of simplification is imposed to the motion equations. This study modifies 6 DOF motion equations to 4+2 DOF motion equations in which heave and pitch equations are replaced by dynamic draught and trim (so-called running attitude), respectively. The method is applicable for a manoeuvre that commences in the planing regime and ends in the same regime. On that basis, the PMM test is conducted and the model is restrained in the vertical plane at a certain running attitude, determined by a resistance test. The 4+2 DOF method, together with MHCs from the PMM test, are employed for the simulation of turning manoeuvres of a 25° prismatic planing hull. The results of the simulation indicate that the 4+2 DOF method reasonably predicts the path of the craft during the turning manoeuvre and cuts the number of PMM tests required at the same time. The PMM test results show that MHCs are highly related to forward speed and wetted surfaces. The turning manoeuvre simulation shows that the non-linear terms of MHCs cannot be ignored. The STD/L (Steady Turning Diameter divided by Length of the craft) for a planing craft is very large, compared to ships.

Keywords: Mathematical modelling, turning manoeuvre, planing craft, 4+2 DOF method, PMM test, planing regime

INTRODUCTION

Planing craft are a kind of high-speed craft whose weights are almost totally supported by the hydrodynamic lift force in the planing regime. This allows them to reach a very high speed. Their small size, in conjunction with very high speed, makes them quite agile compared to ships. For planing craft, the propeller shaft is typically steerable, which plays the role of the rudder. Thus, it provides a very fast steering system to the planing craft. A justified expectation from a fast vessel is a very good manoeuvrability, which is principally true. However, a marginal steering system malfunction, as well as any mishandling by the wheelman, may lead to a high-energy crash and/or vessel capsizing. Thus, the manoeuvrability of planing craft plays a major role in achieving the sufficient level of safety.

An evaluation of ship manoeuvrability usually relies on different methods, such as mathematical formulations, numerical simulations, model experiments and full-scale tests. The mathematical formulation for the manoeuvres includes a system of 3 degrees of freedom (DOF) or 4 DOF motion equations.

NOMENCLATURE

Δ	Mass of planing craft (*kg*)
L	Length overall (*m*)
B	Breadth (*m*)
β	Deadrise angle (*degrees*)
CG	Centre of gravity
LCG	Longitudinal centre of gravity from transom (*m*)
VCG	Vertical centre of gravity from keel (*m*)
I_{xx}	Roll moment of inertia ($kg.m^2$)
I_{zz}	Yaw moment of inertia ($kg.m^2$)
I_{xz}	Yaw-roll moment of inertia ($kg.m^2$)
V	Forward speed (*m/s*)
L_k	Wetted keel length (*m*)
L_c	Wetted chine length (*m*)
Fr	Froude number ($Fr = V/\sqrt{gL}$)
C_v	Speed coefficient ($C_v = V/\sqrt{gB}$)
X	Force in surge direction (*N*)
Y	Force in sway direction (*N*)
K	Moment in roll direction (*N.m*)
N	Moment in yaw direction (*N.m*)
u	Surge velocity (*m/s*)
v	Sway velocity (*m/s*)
$\dot{u}$	Surge acceleration (m/s^2)
$\dot{v}$	Sway acceleration (m/s^2)
ϕ	Roll angle (*degrees or radians*)
θ	Pitch angle (*degrees or radians*)
z	Heave displacement (*m*)
w	Heave velocity (*m*)
$\dot{w}$	Heave acceleration (m/s^2)
p	Roll velocity (*degrees/s* or *radians/s*)
$\dot{p}$	Roll acceleration (*degrees/s*^{2} or *radians/s*^{2})
r	Yaw velocity (*degrees/s* or *radians/s*)
$\dot{r}$	Yaw acceleration (*degrees/s*^{2} or *radians/s*^{2})
X_{thrust}	Thrust force in surge direction (*N*)
Y_{rudder}	Rudder force in sway direction (*N*)
K_{rudder}	Rudder force in roll direction (*N.m*)
N_{rudder}	Rudder force in yaw direction (*N.m*)
$R_t(V)$	Resistance force (*N*)
X_u	Surge force change due to surge velocity change (*N.s/m*)
$X_{\dot{u}}$	Surge force change due to surge acceleration change (*kg*)
X_θ	Surge force change due to pitch motion change (*N*)
X_z	Surge force change due to heave motion change (*N/m*)
X_v	Surge force change due to sway velocity change (N.s/m)
$X_{\dot{v}}$	Surge force change due to sway acceleration change (*kg*)
X_r	Surge force change due to yaw velocity change (*N.s*)
$X_{\dot{r}}$	Surge force change due to yaw acceleration change ($N.s^2$)
X_ϕ	Surge force change due to roll motion change (*N*)
X_p	Surge force change due to roll velocity change (*N.s*)
$X_{\dot{p}}$	Surge force change due to roll acceleration change ($N.s^2$)
Y_v	Sway force change due to sway speed change (*N.s/m*)
$Y_{\dot{v}}$	Sway force change due to sway acceleration change (*kg*)
Y_ϕ	Sway force change due to roll displacement change (*N*)
Y_r	Sway force change due to yaw velocity change (*N.s*)
$Y_{\dot{r}}$	Sway force change due to yaw acceleration change ($N.s^2$)
K_ϕ	Roll moment change due to roll displacement change (*N.m*)
K_p	Roll moment change due to roll velocity change (*N.m.s*)
$K_{\dot{p}}$	Roll moment change due to roll acceleration change ($N.m.s^2$)
K_v	Roll moment change due to sway speed change (*N.s*)
K_r	Roll moment change due to yaw speed change (*N.m.s*)
N_r	Yaw moment change due to yaw speed change (*N.m.s*)
$N_{\dot{r}}$	Yaw moment change due to yaw acceleration change ($N.m.s^2$)
N_ϕ	Yaw moment change due to roll displacement change (*N.m*)
N_v	Yaw moment change due to sway speed change (*N.s*)
$N_{\dot{v}}$	Yaw moment change due to sway acceleration change (*N.m.s*)
f_x	Non-linear terms of hydrodynamic forces in surge direction
f_y	Non-linear terms of hydrodynamic forces in sway direction
f_K	Non-linear terms of hydrodynamic forces in roll direction
f_N	Non-linear terms of hydrodynamic forces in yaw direction

The equations consist of many manoeuvring hydrodynamic coefficients. Generally, MHCs comprise many linear and non-linear force coefficients and some of them are coupling terms. They are mainly determined by captive model tests, empirical formulas and, recently, computational fluid dynamics (CFD)-based simulations. The number of planar motion mechanism test runs for a ship may be as many as two hundred runs (see Yasukawa and Yoshimura [1]). The manoeuvrability of ships is essentially a development issue, where ITTC [2] has already recommended a PMM test procedure for performing model tests.

Many studies have been conducted on the evaluation of manoeuvrability and MHCs extraction of ships using numerical simulations, mathematical models, and experimental and sea-trial approaches. Recently, Sutulo and Soares [3] investigated the available empirical methods for the prediction of ship manoeuvring. They concluded that a general application of universal empirical methods can lead to unacceptably large discrepancies and this method must be used with great care, preferably tuned on prototype ships. Yasuakawa [4] conducted captive model tests for a car carrier in the proximity of a sloped bank with variations in water depth, distances between the ship hull and the bank, hull drift angle and heel angle, to investigate course stability. Taimuri et al. [5] presented a modular mathematical model and a technique for the estimation of manoeuvring trajectories and motion time histories of single and twin-screw propulsion ships, in which MHCs should be extracted from PMM tests or semi-empirical relations. Ni et al. [6] proposed the mathematical model for heave and pitch motion in regular waves to improve the manoeuvring behaviour of a maritime simulator. The multi-parameter conformal mapping method was adopted to solve the hydrodynamic problem of ships' transverse sections The integration of the hydrodynamic coefficients and the wave exciting forces for the ship hull was then obtained using the strip method. Yiew et al. [7] developed a real-time method to simulate vessel manoeuvring in waves. As a benchmark, MHCs of a KCS hull were estimated using URANS-CFD generated manoeuvers in regular waves over a range of incidence angles, wavelengths, and Froude numbers. The estimated wave loads, together with rudder and propeller forces, were prescribed in the mathematical manoeuvring model. Kołodziej and Hoffmann

[8] presented an attempt to develop a computational method for ship manoeuvrability prediction, in which the hydrodynamic characteristics of the hull are identified using a CFD method by simulating the circular motion test.

The running attitude is defined as the draught and trim change of a marine vessel due to forward speed change. Since ships have a negligible running attitude while doing manoeuvres, 4 DOF motion equations (where heave and pitch equations are ignored) effectively simulate their manoeuvrability. However, the running attitude of a planing craft varies as the forward speed changes while doing manoeuvres. Figure 1 depicts a planing craft in a turning manoeuvre in five instants. It is in a steady straight path at a certain speed (V0) and attitude in the planing regime (1). A turning manoeuvre commences by applying the steering force (using a rudder, azimuth thruster, water jet or steerable propeller shaft), and the speed, attitude and path begin to change (2). In the middle of the turn, the speed changes to V1, the attitude proportionally changes and the path follows an arc (3). The craft reaches a steady speed (V2), an appropriate attitude and almost a circular path (4). The steady condition continues to a yaw angle of 180° at the same steady speed of V2 and corresponding attitude (5). The under-water part of the craft rapidly varies, in proportion to the running attitude, which leads to a rapid change in the projected wetted area, as shown in Fig. 1(b). The hydrodynamic forces, due to sway, roll and yaw motions, are related to the projected wetted area. Consequently, 6 DOF motion equations, all of them being coupled to each other, must be employed for a planing craft manoeuvre.

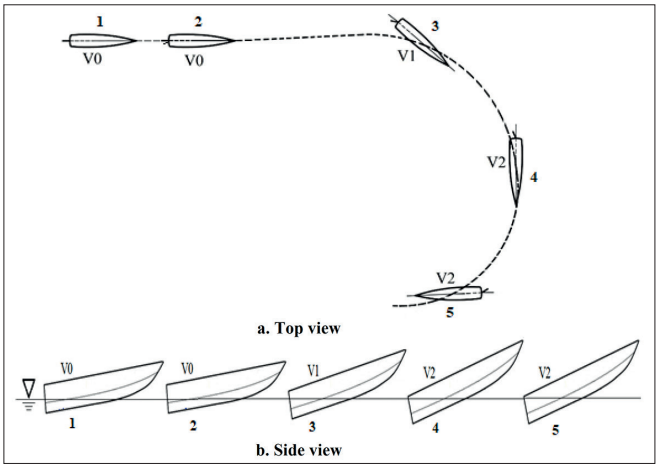

Fig. 1. A scheme of attitude change of a planing craft during turning (1: steady straight path, 2: start of manoeuvre, 3: non-steady path, 4: steady turn, and 5: 180° turning)

Several studies have been conducted on the manoeuvrability of planing craft for the extraction of the MHCs, where the running attitude was taken into consideration as a parameter. Henry [9] investigated hydrodynamic forces in six directions acting on prismatic planing hulls using captive model tests. Henry conducted 863 runs for different conditions of forward speed, trim angle, draught, roll angle, yaw angle and rate.

Plante et al. [10] simulated the manoeuvrability of a craft in the semi-planing regime using the 6 DOF motion equations presented by Toxopeus et al. [11]. The MHCs were extracted using the PMM test, where the model was fully restrained and forced into a manoeuvring motion, and forces were recorded in 6 DOF. The draught, trim angle, forward speed and sway and yaw velocities were systematically varied. They did not consider the roll motion coupling terms and conducted more than 300 test runs. Ikeda et al. [12] did a thorough study of hydrodynamic forces acting on a planing hull for six motions, by conducting 150 to 200 PMM static tests that considered the running attitude, roll angle and yaw angle as the only parameters. Katayama et al. [13] showed that the MHCs of planing hulls are not constant, as they alter as the craft speed changes during a manoeuvre. They concluded that the sway and yaw velocities and accelerations affect the running attitude during manoeuvres. Moreover, the experiments by Katayama et al. [14] on the turning diameter of a planing hull also supported their findings [13]. Katayama et al. [15] presented a 3 DOF mathematical model for the surge, sway and yaw motions during the manoeuvrability of a planing craft in the semi-planing regime. They extracted the MHCs for fixed and free rolling conditions at a certain forward speed but the number of test runs was not reported.

Yasukawa et al. [16] presented 4 DOF motion equations, where the heave and pitch motions were disregarded, for a high-speed ship with a Froude Number from 0.6 to 1.0. They introduced a procedure for the calculation of the MHCs, where running attitude variation was considered with more than 100 test runs for two forward speeds. Ircani et al. [17] simulated the manoeuvrability characteristics of a planing craft by a 4 DOF mathematical model, where the heave and pitch motions were disregarded, based on a captive model test available in the open literature [9,13,14]. Hajizadeh et al. [18] simulated a planing craft manoeuvre by a 4 DOF mathematical model for a straight-line, course-changing and turning manoeuvres, using the MHCs in [19].

Tavakoli and Dashtimanesh [20] simulated a turning manoeuvre for a planing craft using MCHs computed by a 2D+T method [21]. They solved 6 DOF motion equations in a strongly coupled condition. They simulated pure sway and pure yaw tests for two conditions of a fixed and free heave, pitch and roll [21]. Algrin and Bula [22] developed a 6 DOF mathematical model, in conjunction with the 2D+T method, to determine the MHCs. They investigated the influence of the main design parameters, such as the deadrise angle, *LCG*, *VCG* and forward speed, on turning and zigzag manoeuvres.

The above literature review indicates that planing craft manoeuvre simulation requires 6 DOF motion equations to include the running attitude variation. The 6 DOF motion equations require as many as hundreds of MHCs, and each of them needs many experiments; all together, several thousand test runs are required. This is an expensive and time-consuming task, which is a major constraint for the development of planing craft manoeuvre modelling. A solution to this problem is to simplify the motion equations while preserving their generality at the same time. This solution should result in significantly decreasing the number of PMM tests. The present study is an attempt to simplify the motion equations and reduce the number of PMM test runs. An improved accuracy, as well as a reduction in the number of test runs, may be pursued in the introduced method, in the future.

Hence, this study replaces 6 DOF motion equations by 4+2 DOF motion equations, where the '4' refers to surge, sway, roll and yaw motions and '2' refers to a simplified form of heave and pitch motion equations. The simplified heave and pitch equations contain just heave and pitch displacements, and they are equivalent to a dynamic draught and trim that results from the craft's forward speed in a straight path. In other words, the heave and pitch velocities and acceleration-induced forces on the six motions are ignored, due to their relatively marginal effects and to simplify the process. Meanwhile, the coupling between the heave and pitch displacements with four other motions is maintained. Following the 4+2 DOF method, a PMM test procedure is developed. In this procedure, a PMM test at each forward speed is conducted, in which the planing model is restrained for the running attitude that results from a resistance test at the same forward speed. The PMM test must be conducted for a range of forward speeds that the planing craft may encounter during the manoeuvre under consideration. Interpolation of the MHCs between the tested forward speeds is feasible for the rest of the forward speeds.

This study was conducted on a prismatic model with a 25° deadrise angle. Initially, the conventional resistance test was conducted on a range of forward speeds, and the heave and pitch displacements were recorded. Additionally, a set of PMM tests were performed on two forward speeds, which resulted in a set of crucial MHCs. The rest of the MHCs were calculated using a numerical method. Finally, the 4+2 DOF method was employed for a turning manoeuvre simulation, and the result of the simulation was then analysed.

THE 4+2 DOF METHOD

Three coordinate systems are employed to define the planing craft manoeuvre, where the Earth-fixed coordinate system (ECS) and body-fixed coordinate system (BCS) are the same as those for ships [23]; the hydrodynamic coordinate system (HCS) is an additional coordinate system. The HCS contains four motions: three translational motions (surge, sway and heave) and one angular motion (yaw). The origin of this system is always located at the centre of gravity of the planing craft. The ECS, BCS and HCS are denoted by $X_0Y_0Z_0$, $\xi\gamma\zeta$ and xyz, respectively.

Figure 2 shows a trajectory for a planing craft that starts on a straight path at the origin of the ECS, has a forward speed of V_0, and arrives at a new point, where its speed changes to V (a parameter that is composed of u and v and defined in the HCS). The angle between the path of the craft and x-axis is the drift angle, β. The parameter ψ indicates the yaw angle with respect to the heading of the craft at the start of a manoeuvre.

Using Newton's second law in the HCS, the six coupled motion equations for the planing craft manoeuvre can be written as follows [19]:

$$\begin{cases} \Delta\dot{u} - \Delta vr = X \\ \Delta\dot{v} - \Delta ur = Y \\ \Delta\dot{w} = Z \\ I_{xx}\dot{p} - I_{xz}\dot{r} = K \\ I_{yy}\dot{q} = M \\ I_{zz}\dot{r} - I_{xz}\dot{p} = N \end{cases} \quad (1)$$

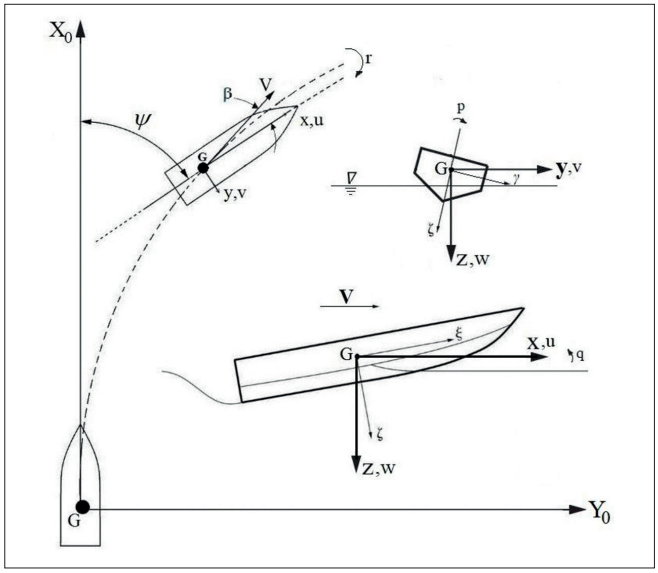

Fig. 2. Definitions of the ECS, BCS and HCS

where X, Y, Z, K, M and N are the hydrodynamic forces of the hull, propeller and rudder in the HCS. The hydrodynamic forces are generated as a result of motion displacements, velocities and accelerations. They may be expressed by first-order or higher-order terms.

Although the heave and pitch strongly affect the four other motions during a manoeuvre, they are marginally affected by the four other motions. As far as the impact of the four other motions on the heave and pitch are concerned, one may conclude (from Sadati et al. [24]) that the yaw, sway and roll velocities are much smaller than the surge velocity during a steady turning manoeuvre. Therefore, the heave and pitch motions are dominated by the surge velocity, which is almost equivalent to the speed of a craft. Additionally, Sadati et al. [24] showed that the trim angle in a straight path is almost equal to the pitch during a steady turning condition in the planing regime.

For the sake of simplicity, the heave and pitch motion equations are replaced by the rise-up and dynamic trim that result from a conventional resistance test, as a function of forward speed. They may also be estimated by a regression method, such as that used by Savitsky [25]. Therefore, this study simplifies the 6 DOF motion equations by introducing 4+2 DOF motion equations that include four dynamic motion equations of surge, sway, roll and yaw and two quasi-static motion equations of heave and pitch. Accordingly, Eq (1) can be rewritten as follows:

$$\begin{cases} \Delta\dot{u} - \Delta vr = X_u u + X_{\dot{u}}\dot{u} + X_\theta\theta + X_z z + X_{thrust} + f_x \\ \Delta\dot{v} - \Delta ur = Y_v v + Y_{\dot{v}}\dot{v} + Y_\phi\phi + Y_p p + Y_{\dot{p}}\dot{p} + Y_r r + Y_{\dot{r}}\dot{r} + Y_{rudder} + f_y \\ z(v): \textit{Extracted from resistance test} \\ I_{xx}\dot{p} - I_{xz}\dot{r} = K_\phi\phi + K_p p + K_{\dot{p}}\dot{p} + K_v v + K_{\dot{v}}\dot{v} + K_r r + K_{\dot{r}}\dot{r} + K_{rudder} + f_k \\ \theta(v): \textit{Extracted from resistance test} \\ I_{zz}\dot{r} - I_{xz}\dot{p} = N_r r + N_{\dot{r}}\dot{r} + N_\phi\phi + N_p p + N_{\dot{p}}\dot{p} + N_v v + N_{\dot{v}}\dot{v} + N_{rudder} + f_N \end{cases} \quad (2)$$

where f_x, f_y, f_k and f_N are non-linear terms for hydrodynamic forces in surge, sway, roll and yaw directions, respectively. The non-linear terms are extracted in the sections following the PMM test results. Effects of the transverse motion (sway-roll-yaw) on the surge motion are ignored, which results in omitting those terms representing transverse forces on f_x (i.e. $X_{vv}v^2$, $X_{\dot{v}\dot{v}}\dot{v}^2$, $X_{rr}r^2$, $X_{\dot{r}\dot{r}}\dot{r}^2$, $X_{\phi\phi}\phi^2$, $X_{pp}p^2$, $X_{\dot{p}\dot{p}}\dot{p}^2$ and the higher orders) [16]. The $X_u u + X_\theta \theta + X_z z$ terms in the surge equation and the non-linear terms in f_x, are replaced by the drag force, measured by a resistance test, $R_t(u)$.

The coupling between the longitudinal and transverse motions is maintained if the MHCs for the surge, sway, roll and yaw motions are related to the forward speed and running attitude. The instantaneous under-water parts of a planing craft are determined by its dynamic draught and trim, which are heave and pitch displacements, respectively. The projected wetted area dominates the hydrodynamic forces for the four other motions, which is why the heave and pitch motions strongly affect them (see Fig. 1(b)). Moreover, to simplify the equations, the coupling between sway, roll and yaw are ignored, which can be considered in future studies.

Following the 4+2 DOF method represented in Eq. (2), a PMM test procedure is developed that requires fewer PMM test runs. In this procedure, a PMM test at each forward speed is conducted in which the planing hull is restrained to the running attitude that results from a resistance test for a given forward speed. The PMM test must be conducted for the range of forward speeds that the planing craft may encounter during the manoeuvre under consideration. Interpolation of the MHCs between the tested forward speeds is achievable for the rest of the forward speeds. A scheme of the 4+2 DOF method and PMM test procedure is illustrated in Fig. 3.

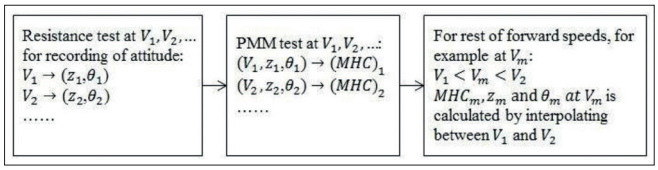

Fig. 3. MHC extraction using PMM test and interpolation following the 4+2 DOF method

PROPULSION AND CONTROL FORCES

Planing craft benefit from surface drive systems, where the control system consists of either a trimmable and steerable propeller or a trimmable propeller together with a conventional rudder (Fig. 4). Figure 5 illustrates the thrust and control forces on a planing craft in a manoeuvre where the trimmable and steerable propeller is employed. The craft has a dynamic trim of τ, and the propeller shaft has a trim of γ and is steered by δR.

According to Fig. 5, the thrust and control force components in the four motion equations of Eq. (2) in HCS may be written as follows:

$$\begin{aligned} X_{thrust} &= T\cos(\gamma+\tau)\cos\delta R \\ Y_{rudder} &= T\cos(\gamma+\tau)\sin\delta R \\ K_{rudder} &= T\cos(\gamma+\tau)\, z_T \sin\delta R \\ N_{rudder} &= T\cos(\gamma+\tau)\, x_T \sin\delta R \end{aligned} \tag{3}$$

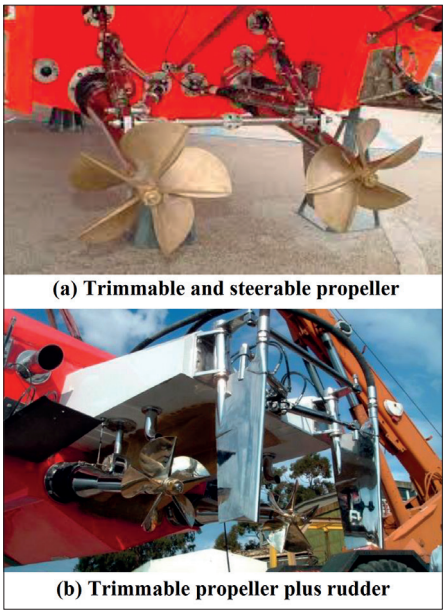

Fig. 4. Steering system of the planing craft [26]

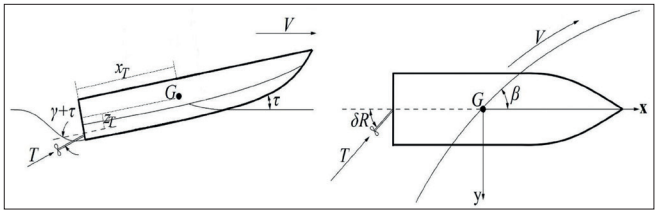

Fig. 5. Thrust and control forces for a surface drive system

where T is the thrust force, and x_T and z_T are x and z coordinates of the thrust force with respect to the centre of gravity, respectively.

MANOEUVRING HYDRODYNAMIC COEFFICIENTS

Following the 4+2 DOF method, a set of PMM test were conducted at the National Iranian Marine Laboratory (NIMALA) for several MHCs. The NIMALA is a well-equipped hydrodynamic laboratory for ships, planing craft and offshore structures; it contains a large towing tank of 400 m length and carriage speed of 18 m/s. It has a PMM that provides the possibility of static and dynamic captive model tests for ships and planing hulls. Due to dynamometer characteristics, the roll induced hydrodynamic coefficients were not recorded. For this study, the PMM tests are employed for MHCs related to sway and yaw velocities and accelerations, and the rest of them are numerically evaluated.

A prismatic planing model is chosen for the simulation. Following Fridsma body lines [27], a model of 25° deadrise angle was selected for the study (Fig. 6). Table 1 shows the main characteristics of the model. It should be noted that the mass moments of inertia are measured in the BCS and are almost equal to the mass moments of inertia in the HCS [19].

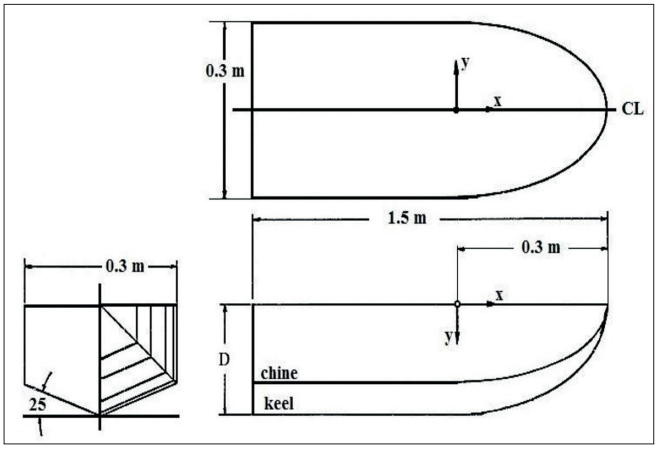

Fig. 6. 25° prismatic model

Tab. 1. Characteristics of the model

Parameter	Value
Deadrise angle	25°
L_{OA}	1.500 (m)
L_{WL}	1.430 (m)
B	0.300 (m)
T	0.376 (m)
LCG from transom	0.615 (m)
Δ	16.450 (kg)
P	1002 (kg/m²)
Radius of gyration	0.375 (m)
$I_{\xi\xi}$	0.160 (kg.m²)
$I_{\zeta\zeta}$	2.313 (kg.m²)

RESISTANCE TEST

Upon considering the 4+2 DOF method given in Eq. (2) and assuming that the hydrodynamic forces of planing hulls are speed dependent, the model is restrained in a vertical plane at a certain attitude. The running attitude of the model, namely the heave and pitch displacements, is determined by conventional resistance testing at a given forward speed. Table 2 shows the results of the resistance tests.

Tab. 2. Results of resistance tests

V (m/s)	Rt (N)	θ (degrees)	z (m)	L_k (m)	L_c (m)
5.00	26.49	3.98	0.01842	1.303	0.452
5.75	28.61	4.14	0.02428	1.274	0.367

PMM TEST

Both static and dynamic PMM tests were conducted at two forward speeds of 5.00 and 5.75 m/s. The model was restrained by the PMM apparatus at fixed running attitudes, as given in Table 2. Table 3 shows the testing scenario and Fig. 7 shows the model during a pure yaw test.

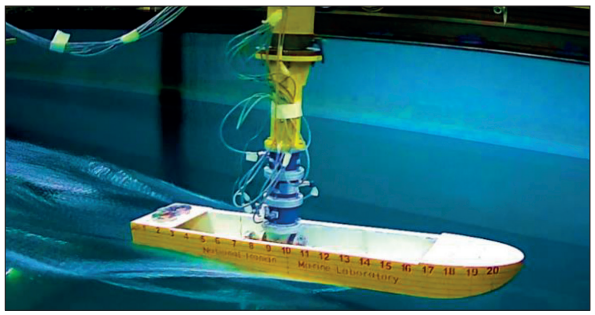

Fig. 7. Model during a pure yaw test

Tab. 3. PMM test scenario

Static drift test		
Forward speed (m/s)	Drift angle (degrees)	Number of tests
5.00 and 5.75	0, ±2, ±4, ±6, ±8 and ±10	20

Pure sway test			
Forward speed (m/s)	Sway amp. (m)	Frequency (Hz)	Number of tests
5.00 and 5.75	0.5	0.15, 0.20, 0.25 and 0.30	8

Pure yaw test				
Forward speed (m/s)	Yaw amp. at V=5 m/s (degrees)	Yaw amp. at V=5.75 m/s (degrees)	Frequency (Hz)	Number of tests
5.00 and 5.75	5.40, 7.20, 9.00 and 10.80	4.70, 6.25, 7.83 and 9.39	0.15, 0.20, 0.25 and 0.30	8

Static drift test

Figure 8 illustrates the results from the static drift tests conducted according to Table 3, at drift angles of 0°, ±2°, ±4°, ±6°, ±8° and ±10°. These drift angles (with respect to $v = -V\sin\beta$) lead to the sway velocities presented in Table 4. As shown in Fig. 6, both the sway force and yaw moment are functions of sway velocity which follow a non-linear curve that corresponds to the cubic polynomial, resulting in Y_v, Y_{vvv}, N_v and N_{vvv}.

Tab, 4. The sway velocity in static drift test

Forward Speed (m/s)	Drift angle (degrees)	Sway velocity (m/s)
5.00	0, ±2, ±4, ±6, ±8 and ±10	0, ±0.175, ±0.349, ±0.523, ±0.696 and ±0.868
5.75	0, ±2, ±4, ±6, ±8 and ±10	0, ±0.201, ±0.401, ±0.601, ±0.800 and ±0.998

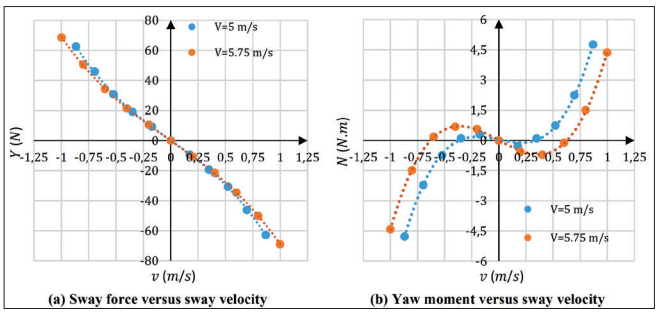

Fig. 8. Static drift force at two forward speeds

Pure sway test

Referring to Table 3, the pure sway test was conducted at oscillation frequencies of 0.15, 0.20, 0.25 and 0.30 Hz and a sway amplitude of 0.5 m, resulting in the sway acceleration given in Table 5. Figure 9 illustrates the pure sway test results as a function of sway acceleration. The sway force is almost a linear function of the sway acceleration, which results in the linear term $Y_{\dot{v}}$. Following the curve fitting, the yaw moment is a third-degree polynomial function of the sway acceleration, which yields $N_{\dot{v}}$ and $N_{\dot{v}\dot{v}\dot{v}}$.

Tab. 5. The sway acceleration in pure sway test

Forward Speed (m/s)	Sway amp. (m)	Frequency (Hz)	Sway acceleration (m/s²)
5.00	0.5	0.15, 0.20, 0.25 and 0.30	±0.444, ±0.790, ±1.234, ±1.777
5.75	0,5	0.15, 0.20, 0.25 and 0.30	±0.444, ±0.790, ±1.234, ±1.777

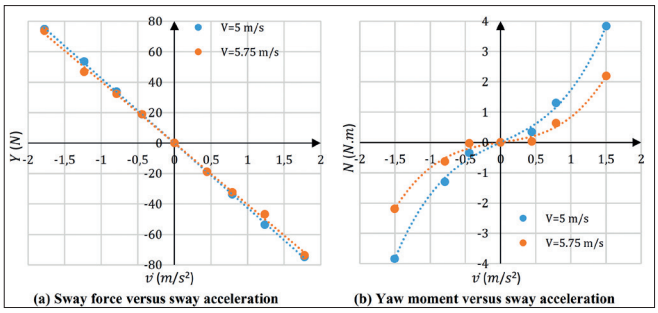

Fig. 9. Pure sway test at two forward speeds

Pure yaw test

Regarding Table 3, the pure yaw test is conducted at a sway amplitude of 0.5 m, frequencies of 0.15, 0.20, 0.25 and 0.30 Hz and yaw amplitudes of 4.70°, 6.25°, 7.83° and 9.39°. The tests were conducted at the yaw velocities and accelerations shown in Table 6. Figure 10 demonstrates the yaw velocity induced forces on the sway and yaw motions. Using curve fitting, the sway force and yaw moment are third-degree polynomial functions of the yaw velocity.

Tab. 6. The yaw velocity and acceleration in pure yaw test

Forward Speed (m/s)	Frequency (Hz)	Yaw amp. (degrees)	Yaw velocity (m/s)	Yaw acceleration (m/s²)
5.00	0.15, 0.20, 0.25 and 0.30	5.40, 7.20, 9.00 and 10.80	±0.089, ±0.158, ±0.247 and ±0.355	±0.084, ±0.198, ±0.388 and ±0.670
5.75	0.15, 0.20, 0.25 and 0.30	4.70, 6.25, 7.83 and 9.39	±0.077, ±0.137, ±0.215 and ±0.309	±0.073, ±0.172, ±0.337 and ±0.582

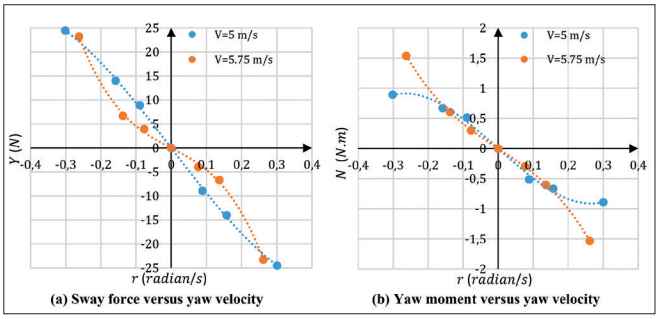

Fig. 10. Pure yaw test for yaw velocity at two forward speeds

Figure 11 presents the sway force and yaw moment versus the yaw acceleration. The yaw moment is approximated as a linear function of the yaw acceleration, i.e. $N_{\dot{r}}$. Through curve fitting, the sway force is approximated by a cubic polynomial of the yaw acceleration, i.e. $Y_{\dot{r}}$ and $Y_{\dot{r}\dot{r}\dot{r}}$.

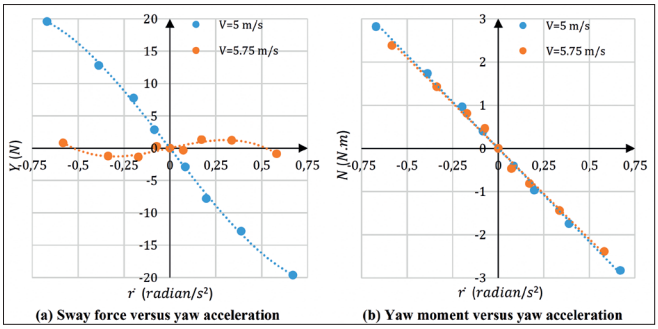

Fig. 11. Pure yaw test for yaw acceleration at two forward speeds

MHCs calculated from the PMM test

Following the above details, the MHCs induced by the sway and yaw velocities and accelerations are summarised in Table 7.

Tab. 7. MHCs for the 25o prismatic model calculated from the PMM tests

No.	MHC	Dimension	V=5.00 (m/s)	V=5.75 (m/s)
1	Y_{v}	N.s/m	-52.1660	-51.0590
2	Y_{vvv}	N.s³/m³	-26.9240	-18.0090
3	N_{v}	N.s	-1.0858	-2.8983
4	N_{vvv}	N.s³/m²	8.7667	7.3440
5	$Y_{\dot{v}}$	kg	-26.0970	-24.0040
6	$N_{\dot{v}}$	N.s²	1.0705	0.3437
8	$N_{\dot{v}\dot{v}\dot{v}}$	N.s³/m²	0.6579	0.4941
9	Y_{r}	N.s	-12.7850	56.2585
10	Y_{rrr}	N.s³	152.1700	-731.8400
11	N_{r}	N.m.ˢ	-5.1717	-3.8114
12	N_{rrr}	N.m.s³	24.5950	-29.9710
13	$Y_{\dot{r}}$	N.s²	-36.5520	6.2713
14	$Y_{\dot{r}\dot{r}\dot{r}}$	N.s⁶	16.4030	-22.7920
15	$N_{\dot{r}}$	N.m.s²	-2.0112	-1.8862

ROLL INDUCED MHCS

Slender body theory may be utilised for the evaluation of certain MHCs. Referring to Sadati et al. [28], Appendix 1 presents the principles and the formulas for the calculation of MHCs for two-dimensional wedge sections, using the water entry problem for the asymmetric wedges. Based on Appendix 1, a computer code was developed, where the inputs are V, L_k, β, ϕ, and θ, and the outputs are the roll-induced forces on the sway, roll and yaw motions, e.g. Y_{ϕ}, N_{ϕ}, K_{ϕ} and their higher orders, respectively. The computer code is employed for the 25° prismatic model at roll angles of 0°, ±2°, ±4°, ±6°, ±8° and ±10° at forward speeds of 5.00

and 5.75 m/s. Figure 12 shows the roll induced sway force, roll moment and yaw moment as a function of the roll angle. Table 8 shows the calculated MHCs at two forward speeds. As shown, the linear term reasonably represents the considered MHCs in the model over a practical range of roll angles (less than 10°).

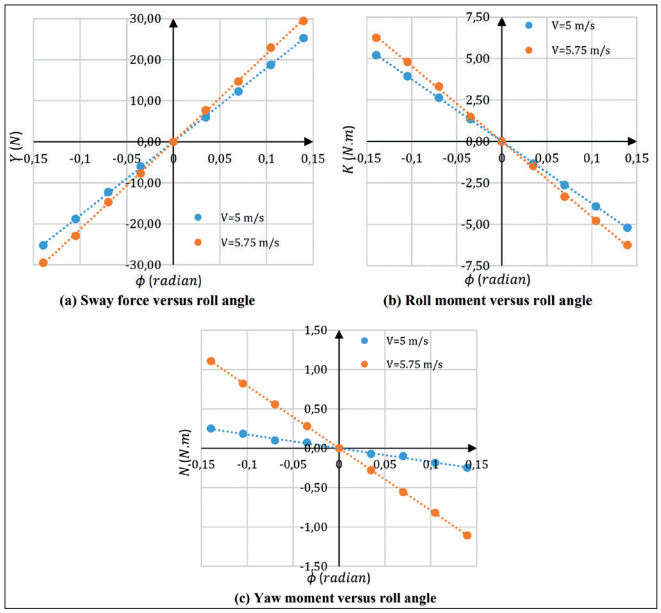

Fig. 12. Roll angle induced forces using the 2D+T method at two forward speeds

Tab. 8. Roll angle induced MHC for the 25° prismatic model

No.	MHC	Dimension	V=5.00 (m/s)	V=5.75 (m/s)
1	Y_ϕ	N/rad	179.3700	213.6900
2	K_ϕ	N.m/rad	-37.3890	-45.3740
3	N_ϕ	N.m/rad	-1.7382	-7.9092

SIMULATION OF THE TURNING MANOEUVRE USING THE 4+2 DOF METHOD

Simulation of the turning manoeuvre based on the 4+2 DOF method requires a computer code, all MHC terms and the propulsion and control forces. In this section, they are considered for the 25° prismatic model. A computer code is developed based on the procedure shown in Fig. 13.

MHCS

To simulate a turning manoeuvre, many MHCs are required; several of them are calculated from experiments and the 2D+T method, as described in the previous section. The rest of them are collected from other applicable studies. Zeratagar et al. [29] tested the same 25° prismatic model and reported the surge added massfor 1.454 and 1.222 kg at forward speeds of 5.00 and 5.75 m/s, respectively. Lewandowski [19] suggested regression equations for a set of roll-induced MHCs, such as K_p, $K_{\dot{p}}$ and K_v where Y_p, $Y_{\dot{p}}$, N_p, $N_{\dot{p}}$, $K_{\dot{v}}$, K_r and $K_{\dot{r}}$ were regarded as being zero. The surge added mass anticipated by Zeratagar et al. [29] and some of the roll induced MHCs, estimated by Lewandowski [19], are employed in the simulation.

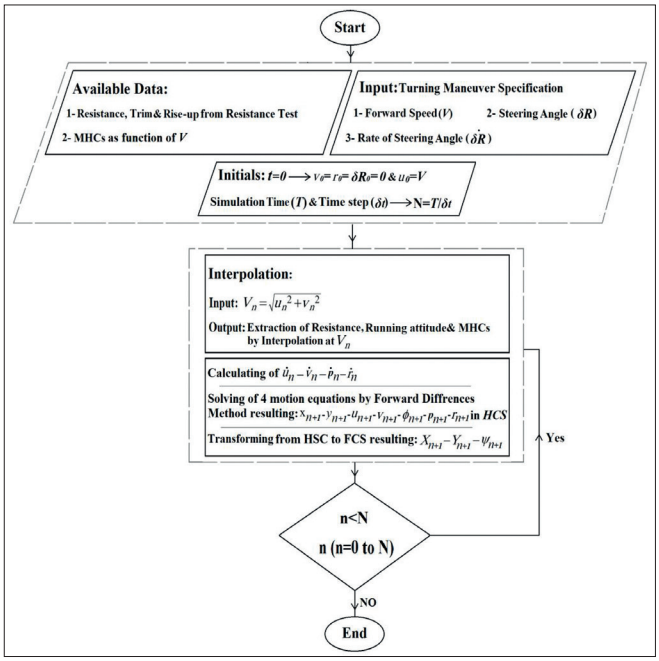

Fig. 13. Simulation Procedure

ACCOMPLISHED MANOEUVRE MOTION EQUATIONS FOR THE 4+2 DOF METHOD

The PMM tests and 2D+t method, along with the available MHCs from the literature, provided a set of linear and non-linear MHCs. It should be noted that the motion equations based on Newton's second law are written for linear accelerations. Therefore, the non-linear terms of MHCs due to acceleration are considered to be zero in the motion equations. Following the results and analysis from the PMM tests and simulations, non-linear terms for the MHCs, namely f_x, f_y, f_k and f_N, are given in Table 7 and 8. Finally, the 4+2 DOF motion equations are as follows:

$$\begin{cases} \Delta\dot{u} - \Delta vr = R_t(u) + X_{\dot{u}}\dot{u} + T\cos(\gamma+\tau)\cos\delta R \\ \Delta\dot{v} - \Delta ur = Y_v v + Y_{vvv}v^3 + Y_{\dot{v}}\dot{v} + Y_\phi\phi + Y_p p + Y_{\dot{p}}\dot{p} + Y_r r + Y_{rrr}r^3 + Y_{\dot{r}}\dot{r} + T\cos(\gamma+\tau)\sin\delta R \\ z(v): \textit{Extracted from resistance test} \\ I_{xx}\dot{p} - I_{xz}\dot{r} = K_\phi\phi + K_p p + K_{\dot{p}}\dot{p} + K_v v + K_{\dot{v}}\dot{v} + K_r r + K_{\dot{r}}\dot{r} + T\cos(\gamma+\tau)z_T\sin\delta R \\ \theta(v): \textit{Extracted from resistance test} \\ I_{zz}\dot{r} - I_{xz}\dot{p} = N_r r + N_{rrr}r^3 + N_{\dot{r}}\dot{r} + N_\phi\phi + N_p p + N_{\dot{p}}\dot{p} + N_v v + N_{vvv}v^3 + T\cos(\gamma+\tau)x_T\sin\delta R \end{cases} \quad (4)$$

RESULTS AND DISCUSSION

A computer code was developed in MATLAB software, according to an algorithm, as per Fig. 13 and Eq. (4). It should be noted that the non-linear terms in Eq. (4) are particularly applicable to the 25° prismatic model. For any new planing craft, they must be determined appropriately.

Simulation of a turning manoeuver with the 25° prismatic model

A turning manoeuvre for the 25° prismatic model was simulated. It commenced with the model moving in a straight path at a forward speed of 5.75 m/s (Fr = 1.5) in a steady condition. It continued by changing the steering angle to 10° with a rate of 1.5 degrees/s. Figure 14 depicts the trajectory of the model in the ECS. The STD is about 29.5 m, which is equal to a STD/L of 19.66, which is relatively large in comparison to that for ships.

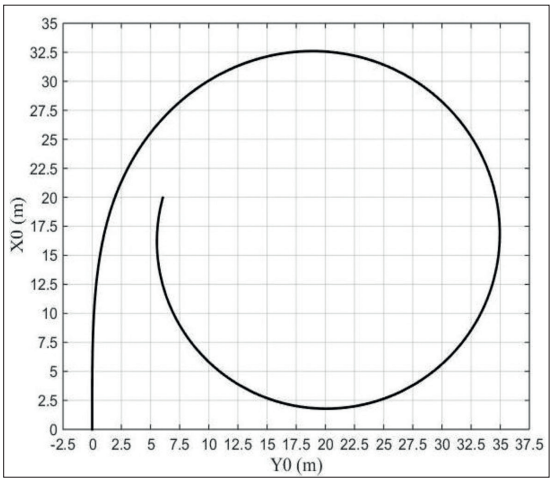

Fig. 14. Turning manoeuvre trajectory at 5.75 m/s and steering angle of 10°

Figure 15 shows the surge acceleration and velocity versus time. The surge encounters a sharp deceleration in 7 s. Then, it smoothly returns to zero, as expected. This indicates that the steering force is dominant for the planing craft, in contrast to the situation for ships. After a while, the surge velocity starts to diminish, and it finally becomes steady after 50 s. The surge velocity reduces about 0.54 m/s during the turning manoeuvre. One should note that the calculation assumes that the propulsion system provides a constant net thrust during the turning manoeuvre.

Figure 16 depicts the sway velocity and acceleration versus time. The 25° prismatic model transversely accelerates and reaches its maximum value after 3 s as the steering force rapidly generates and then quickly returns to zero. The sway velocity follows the acceleration tendency and starts from zero when the manoeuvre commences, and approaches -0.17 m/s in its steady condition. The sway motion comes to a steady condition as early as 30 s after the start of the manoeuvre.

Figure 17 illustrates the yaw velocity and acceleration versus time. They follow the same trend as the sway velocity and acceleration. In the steady condition, the yaw velocity reaches 21.7 degrees/s, while the yaw acceleration reaches zero. Figure 18 shows the roll angle versus time. The roll angle starts at zero and reaches 6.8° at the steady condition.

Figure 19(a) shows the forward speed, V, versus time. It loses 0.545 m/s of its initial value and reaches 5.205 m/s after 35 s. Figure 19(b) shows the drift angle, β, versus time. The drift

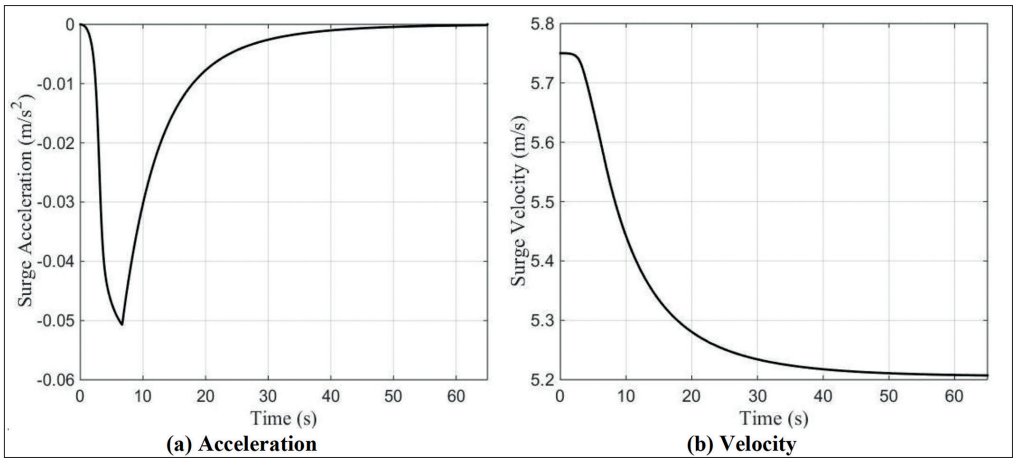

Fig. 15. Surge velocity and acceleration versus time

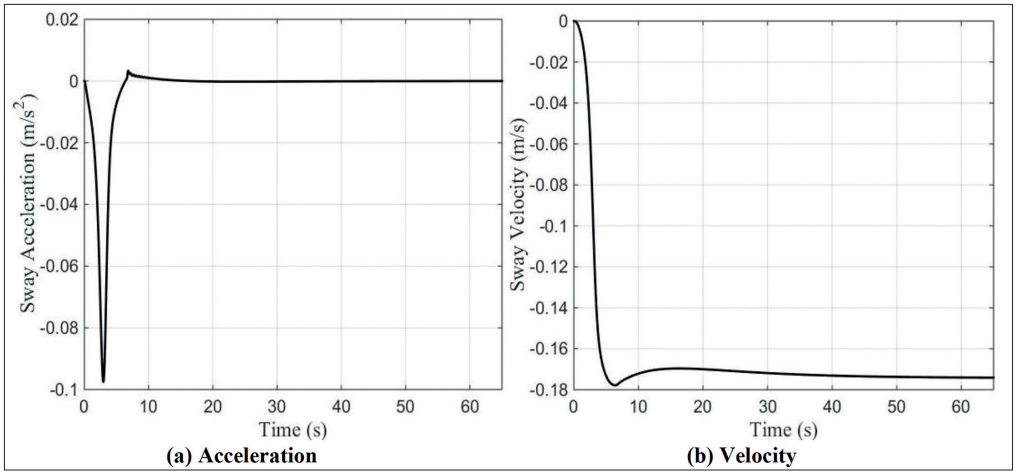

Fig. 16. Sway velocity and acceleration versus time

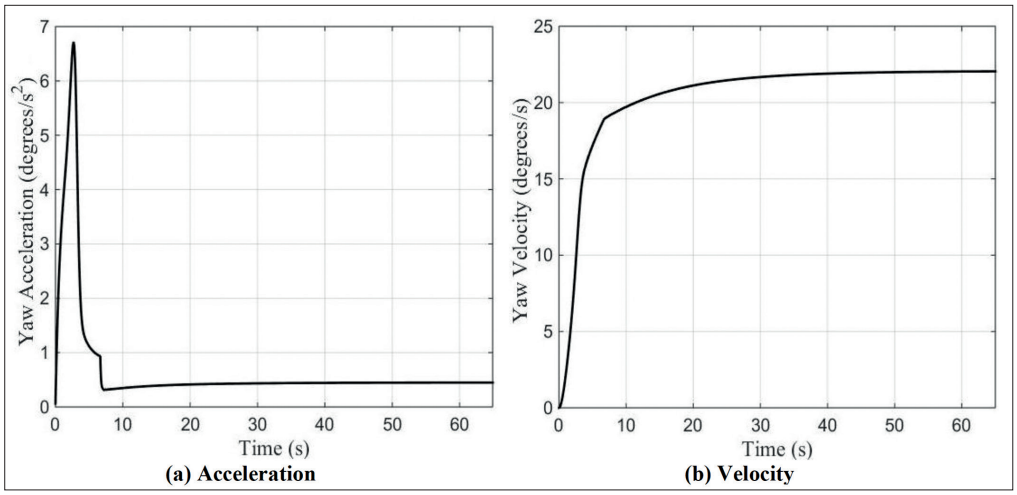

Fig. 17. Yaw velocity and acceleration versus time

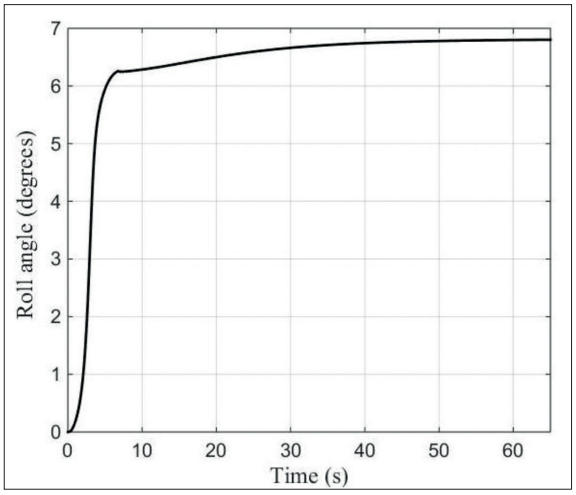

Fig. 18. Roll angle versus time

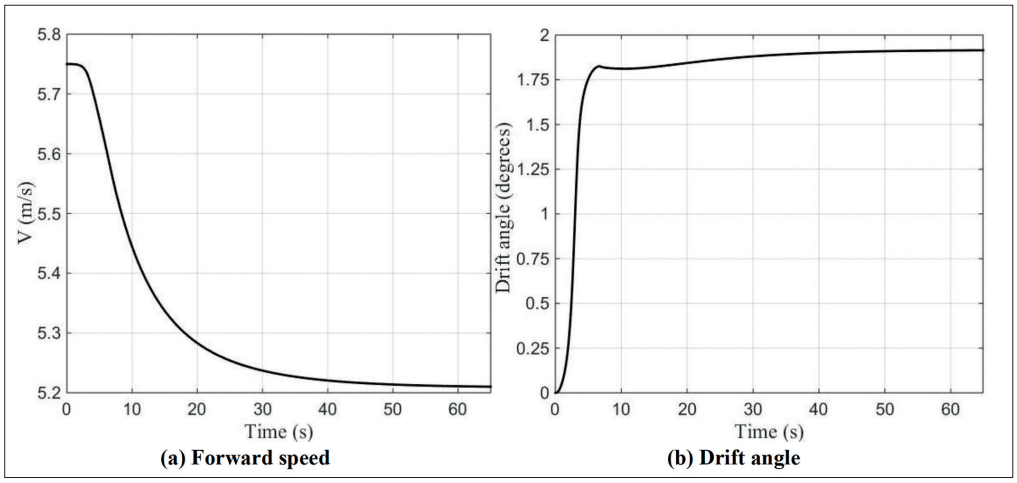

Fig. 19. Forward speed (a) and Drift angle (b) versus time

angle starts at zero and approaches 1.9°. It seems that the drift angle reaches the steady condition after 40 s.

It can be seen that all displacements and velocities reach constant values, while the acceleration becomes zero in the steady turning condition.

Effects of non-linear MHC terms on the turning parameters

For most physical phenomena, linear terms play the main role and justify ignoring non-linear terms. If non-linear terms are disregarded, the simulation is simplified and requires less

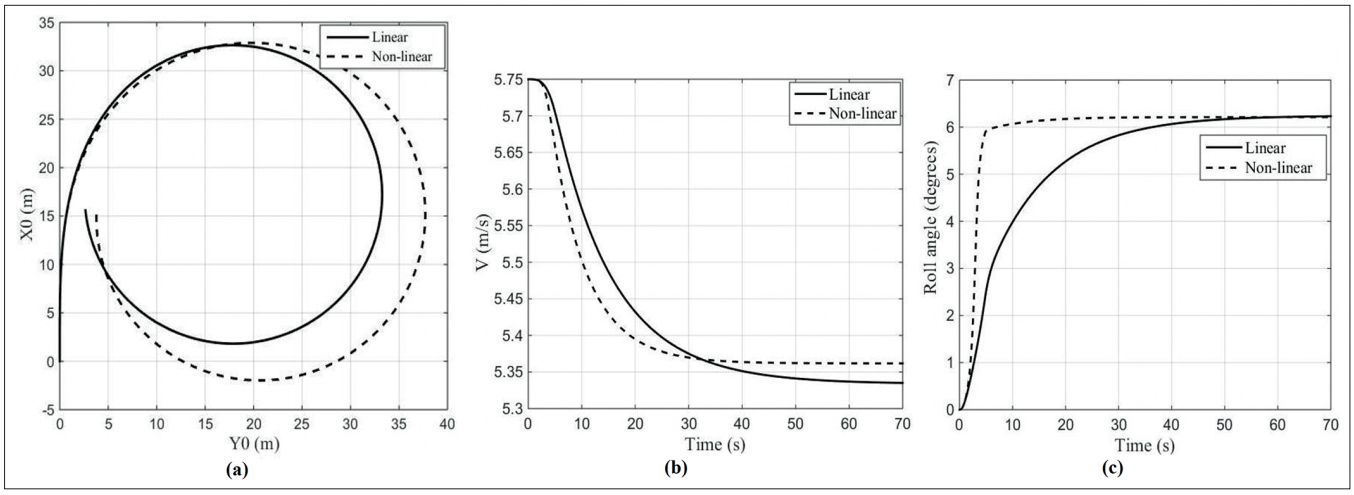

Fig. 20. Effects of non-linear MHC terms on the turning manoeuvre at 5.75 m/s and steering angle of 7°

effort. To investigate the significance of non-linear terms on the simulation results, the simulation was repeated with linear MHC terms only. Figure 20 compares the results of the linear and non-linear simulations at a forward speed of 5.75 m/s, steering angle of 7° and steering angle rate of 1.5 degrees/s. Although the considered steering angle is relatively small, the influence of the non-linear MHCs on the turning manoeuvres was significant.

Verification

Verification of a simulation is typically achieved by comparing the results with those from manoeuvring trials of full-scale boats or a free-running model test. The prismatic models, such as the 25° deadrise angle in this study, are benchmark hulls that have never been built as a planing boat. Additionally, a free-running model test of a planing boat is almost impossible, due to the need for a relatively large engine that is hard to accommodate in the model. The only solution is to conduct full-scale manoeuvring trials with an existing planing boat, to qualitatively verify the simulation results.

We conducted full-scale manoeuvring tests on two boats (Case A and Case B) and the results have recently been published [24]. The boat in case A had a length of 15.4 m and a weight of 11.0 tons. It is not possible to find out whether full-scale test runs fully complied with the simulations and of the several test runs, two of them were selected for qualitative verification; they were more compliant with the model data. The tests started at a forward speed of 38.5 knots (Fr = 1.61) and rudder angles of 14° and 20°. The trajectories of the turning manoeuvre are illustrated in Fig. 21, where the STD/L was 34.00 and 17.80 at a rudder angle of 14° and 20°, respectively. The forward speed decreased to 34.00 and 30.00 knots at a rudder angle of 14° and 20°, respectively [24].

The boat in Case B had a length of 7.9 m and a weight of 3.0 tons. One of the turning tests of Case B starts and ends in the planing regime. The test starts at a forward speed of 36.5 knots (Fr = 2.13) and rudder angle of 10°. Figure 22 shows the path of the turning manoeuvre where STD/L was 34.9. The forward speed decreased from 36.50 knots to 29.5 knots [24].

Despite the dissimilarities between the 25° prismatic model and planing boats, in terms of geometries and control systems, an inherent similarity may be observed by comparing Fig. 13 with Fig. 21 and 22. It may be concluded that the full-scale manoeuvring trials qualitatively support the 4+2 DOF method.

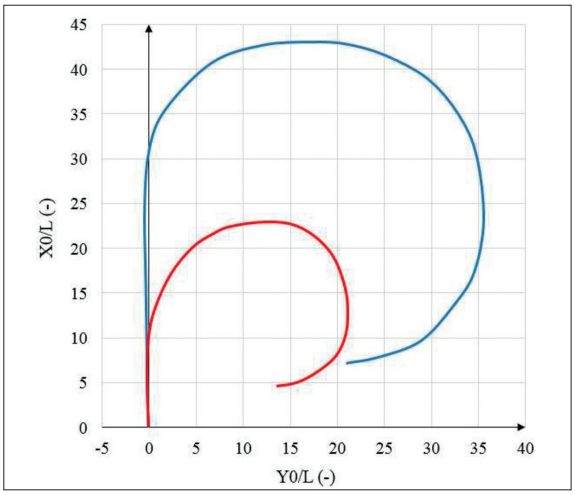

Fig. 21. Non-dimensional path of turning manoeuvre of Case A at rudder angles of 14° (blue) and 20° (red) [24]

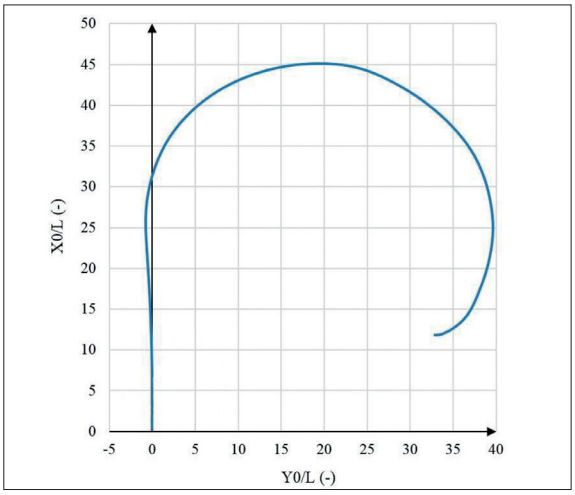

Fig. 22. Non-dimensional path of turning manoeuvre of Case B at rudder angle of 10° [24]

CONCLUSIONS

In this study, standard 6 DOF motion equations for planing craft manoeuvres are developed in the form of 4+2 DOF motion equations, including heave and pitch motions in a simplified form, to ease the simulation requirements. The developed method is applicable for those simulations which commence in the planing regime and ends in the same regime. Based on the 4+2 DOF method, a PMM test set-up is developed and conducted on a 25° prismatic hull. The conclusions of this study are as follows:

- The 4+2 DOF method effectively simplifies planing craft manoeuvre simulations and decreases the number of PMM tests.
- According to PMM test results, MHCs are highly related to forward speed and wetted surfaces.
- The non-linear terms of MHCs cannot be ignored for simulation of manoeuvrability.
- The STD/L for a planing craft is very large (about 30), compared to ships (about 5), if the turning manoeuvre is conducted in the planing regime and ended in the same regime.

REFERENCES

1. H. Yasukawa and Y. Yoshimura, "Introduction of MMG standard method for ship manoeuvering predictions", Journal of Marine Science and Technology, Vol. 20, pp. 37–52, 2015, (DOI: https://doi.org/10.1007/s00773-014-0293-y).

2. ITTC manoeuvring group members, "Testing and extrapolation methods, manoeuvrability captive model test procedures", ITTC–Recommended. 7.5-02-06–02, Revision 02, 2008.

3. S. Sutulo and G. Soares, "On the application of empiric methods for prediction of ship manoeuvring properties and associated uncertainties", Journal of Ocean Engineering, Vol. 186, 2019, (DOI: https://doi.org/10.1016/j.oceaneng.2019.106111).

4. H. Yasukawa, "Manoeuvering hydrodynamic derivatives and course stability of a ship close to a bank", Journal of Ocean Engineering, Vol. 188, 2019, (DOI: https://doi.org/10.1016/j.oceaneng.2019.106149).

5. G. Taimuri, J. Matusiak, T. Mikkola, P. Kujala and S. Hidaris, "A 6-DoF manoeuvring model for the rapid estimation of hydrodynamic actions in deep and shallow waters", Journal of Ocean Engineering, Vol. 218, 2020, (DOI: https://doi.org/10.1016/j.oceaneng.2020.108103).

6. S. Ni, Z. Liu, Y. Cai and T. Zhang, "A practical approach to numerically predicting a manoeuvring vessel in waves oriented to maritime simulator", Journal of Mathematical Problems in Engineering, Article ID 8361951, 2020, (DOI:10.1155/2020/8361951).

7. L. Yiew, Y. Jin and A. Magee, "A practical approach to numerically predicting a manoeuvring vessel in waves oriented to maritime simulator", Journal of Physics: Conf. Series, 1357, 2019, (DOI: https://doi.org/10.1155/2020/8361951).

8. R. Kołodziej and P. Hoffmann, "Numerical Estimation of Hull Hydrodynamic Derivatives in Ship Manoeuvring Prediction", Polish Maritime Research, Vol. 28, pp. 46-53, 2021.

9. C.J. Henry, "Calm water equilibrium, directional stability and steady turning conditions for recreational planing crafts", Davidson Laboratory, Stevens Institute of Technology report No. CG-D-8-76, 1976.

10. M. Plante, S.L. Toxopeus, J. Blok and J.A. Keuning, "Hydrodynamic manoeuvring aspects of planing craft", International Symposium and Workshop on Forces Acting on a manoeuvring Vessel, Val de Reuil, France, 1998.

11. S.L. Toxopeus, J.A. Keuning and J.P. Hooft, "Dynamic stability of Planing Ships, International Symposium and Seminar on the Safety of High Speed Craft", RINA, London, 1997.

12. Y. Ikeda, T. Katayama and H. Okumura, "Characteristics of hydrodynamic derivatives in manoeuvring equations for super high-speed planing hulls", Proceedings of the 10th International Offshore and Polar Engineering Conference, 2000.

13. T. Katayama, R. Kimoto and Y. Ikeda, "Effects of running attitudes on manoeuvring hydrodynamic forces for planing hulls", 5th International Conference on Fast Sea Transportation, FAST, St. Petersburg, Russia, 2005.

14. T. Katayama, T. Iida and Y. Ikeda, "Effects of change in running attitude on turning diameter of planing craft", Proceedings of 2nd PAAMES and AMEC, Jeju Island, Korea, 2006.

15. T. Katayama, T. Taniguchi, H. Fuji and Y. Ikeda, "Development of manoeuvring simulation method for high speed craft using hydrodynamic forces obtained from model test", 10th International Conference on Fast Sea Transportation, FAST, Athens, Greece, 2009.

16. H. Yasukawa, N. Hirata and Y. Nakayama, "High-Speed Ship Manoeuvrability", Journal of Ship Research, Vol. 60 (4), pp. 239-258, 2016, (DOI: https://doi.org/10.5957/JOSR.60.4.160032).

17. A. Ircani, M. Martelli, M. Viviani, M. Altosole, C. Podenzana-Bonvino and D. Grassi, "A simulation approach for planing boats propulsion and manoeuvrability", Transaction RINA, International Journal of Small Craft Technology, Vol.158 (Part B1), 2016, (DOI:10.3940/rina.ijsct.2016.b1.180).

18. S. Hajizadeh, M.S. Seif and H. Mehdigholi, "Evaluation of planing craft manoeuvrability using mathematical modelling

under the action of the rudder", Journal of Scientia Iranica, Vol. 24 (1), pp. 293-301, 2017, (DOI: 10.24200/SCI.2017.4033).

19. E.M. Lewandowski, "The Dynamics of Marine Craft: Manoeuvring and Seakeeping", Advanced Series on Ocean Engineering, 22, World Scientific Publishing Co. Pte. Ltd., Singapore, 2004.

20. S. Tavakoli and A. Dashtimanesh, "A six-DOF theoretical model for steady turning manoeuver of a planing hull", Journal of Ocean Engineering, Vol. 189, 2019, (DOI: https://doi.org/10.1016/j.oceaneng.2019.106328).

21. S. Tavakoli and A. Dashtimanesh, "Mathematical simulation of planar motion mechanism test for planing hulls by using 2D+T theory", Journal of Ocean Engineering, Vol. 169, pp. 651-672, 2018, (DOI: https://doi.org/10.1016/j.oceaneng.2018.09.045).

22. R. Algarin and A. Bula, "A numeric study of the manoeuvrability of planing hulls with six degrees of freedom", Journal of Ocean Engineering, Vol. 221, pp. 1-16, 2021, (https://doi.org/10.1016/j.oceaneng.2020.108514).

23. E.V. Lewis, "Volume III of principles of naval architecture, motion in waves and controllability", The Society of Naval Architects and Marine Engineering, revision 02, 1989.

24. K. Sadati, H. Zeraatgar and A. Moghaddas, "Investigation of planing craft manoeuvrability using full-scale tests", Proceedings of the Institution of Mechanical Engineers Part M Journal of Engineering for the Maritime Environment, 2022, (DOI: doi/abs/10.1177/14750902211030386).

25. D. Savitsky, "Hydrodynamic design of planing hulls", Journal of Marine Technology, Vol. 32 (3), pp 78-88, 1964.

26. Topsystemdrive.com.

27. G. Fridsma, "A systematic study of the rough-water performance of planing boats", Davidson Laboratory, Stevens Institute of Technology report No. 1275, 1969.

28. K. Sadati, H. Zeraatgar and S. Babuei, "Roll hydrodynamic coefficients of planing craft's manoeuver using 2D+t approach", Journal of Scientia Iranica, Vol. 29, Issue 3, pp. 1197-1209, 2022, (DOI: 10.24200/sci.2021.57379.5208).

29. H. Zeraatgar, A. Moghaddas and K. Sadati, "Analysis of surge added mass of planing hulls by model experiment", Journal of Ships and Offshore Structures, Vol. 15 (3), pp. 310-317, 2019, (DOI: https://doi.org/10.1080/17445302.2019.1615705).

30. O. Tascon, A. Troesh and K. Maki, "Numerical computation of the hydrodynamic forces acting on a manoeuvering planing hull via slender body theory-SBT and 2-D impact theory", 10th International Conference on Fast Sea Transportation, FAST, Athens, Greece, 2009.

31. M. Morabito, "Prediction of planing hull side forces in yaw using slender body oblique impact theory", Journal of Ocean Engineering, Vol. 101, pp. 47-57, 2015, (https://doi.org/10.1016/j.oceaneng.2015.04.014).

32. R. Algarin and O. Tascon, "Hydrodynamic modelling of planing boats with asymmetry and steady condition", IX HSMV, Naples, 2011.

33. Y. Toyama, "Two dimensional water impact of unsymmetrical bodies", Journal of the Society of Naval Architects of Japan, Vol. 173, pp. 285-291, 1993, (DOI: https://doi.org/10.2534/jjasnaoe1968.1993.285).

APPENDIX 1

FORMULATION OF ROLL INDUCED MHCS USING WATER ENTRY FOR 2-D WEDGE SECTIONS AND THE SLENDER BODY METHOD

Several studies were undertaken for the calculation of MHCs, based on the slender body method. Tascon et al. [30] studied the application of the slender body method for the computation of hydrodynamic forces acting on a planing hull. They utilised commercial CFD software, Star CCM+®, to obtain the force distribution on a rolled wedge impacting the water surface and having vertical and horizontal velocities. Then, the forces on the two-dimensional wedge sections were integrated along the length of the craft, which resulted in the hydrodynamic forces. Morabito [31] employed a two-dimensional oblique impact model on a three-dimensional planing body using the slender body theory for an estimation of the planing hull side force as a function of the sway velocity.

Following the above methods, a static roll test was simulated for the calculation of Y_ϕ, K_ϕ and N_ϕ, based on a solution for an asymmetric water entry for the 2-D wedges. The problem considered here is the roll displacement, ϕ, and induced hydrodynamic forces on the sway, roll and yaw motion. Algarin and Tascon [33] considered the water entry problem for 2-D wedges at a vertical speed of w and acceleration of $\dot{w}$ at the asymmetric condition defined in Figure 1. The pressure on each side of the wedge is as follows:

$$\frac{P}{\rho} = \dot{w}\sqrt{C^2-(-\mu+y)^2} + \frac{w\left(C\dot{C}+(-\mu+y)\dot{\mu}\right)}{\sqrt{C^2-(-\mu+y)^2}} - \frac{w^2}{2}\frac{-(-\mu+y)^2}{C^2-(-\mu+y)^2} \tag{1}$$

where c and $\dot{c}$ are the wetted beam and its rate, respectively. Also, μ and $\dot{\mu}$ are defined as asymmetric parameters and their rates, as follows [33]:

$$\begin{cases} \mu = \frac{1}{2}(C_1 - C_2) \\ \dot{\mu} = \frac{1}{2}(\dot{C}_1 - \dot{C}_2) \end{cases} \tag{2}$$

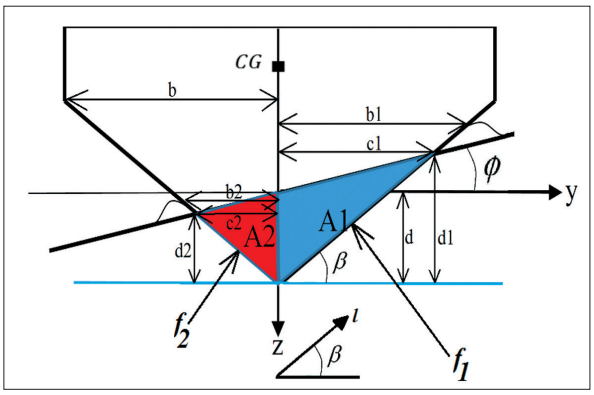

Figure 1. Definition of parameters for the water entry problem for a wedge in an asymmetric condition.

For a planing craft during rolling, each section may face three conditions: un-wetted chine of both sides; wetted chine of one side and un-wetted chine of the other side; and wetted chine of both sides. As a chine becomes wet, the term $\dot{w}$ decreases to zero, the pressure at the chine decreases to zero and Eq (1) is modified accordingly. At a given pair of forward speeds and roll angles, each section along the wetted keel length (L_k) is determined as a chine with a wetted or un-wetted section. The pressure evaluated by Eq (1) is integrated around both sides of a section and forces, f_1 and f_2, and the centre of forces, y_{c1}, y_{c2}, z_{c1} and z_{c2}, are calculated as follows:

$$f_1 = \int_0^{b_1/cos\beta} P.dl \quad \text{and} \quad f_2 = \int_0^{b_2/cos\beta} P.dl \tag{3}$$

$$y_{c1} = \frac{\int_0^{b_1/cos\beta} Pl.dl}{f_1} cos\beta \quad \text{and} \quad y_{c2} = \frac{\int_0^{b_2/cos\beta} Pl.dl}{f_2} cos\beta \tag{4}$$

$$z_{c1} = \frac{\int_0^{b_1/cos\beta} Pl.dl}{f_1} sin\beta \quad \text{and} \quad z_{c2} = \frac{\int_0^{b_2/cos\beta} Pl.dl}{f_2} sin\beta \tag{5}$$

$$\vec{f} = \vec{f}_1 + \vec{f}_2 \tag{6}$$

$$f_{y1} = -f_1 sin\beta \quad \text{and} \quad f_{y2} = -f_2 sin\beta \tag{7}$$

$$f_{z1} = -f_1 cos\beta \quad \text{and} \quad f_{z2} = -f_2 cos\beta \tag{8}$$

$$m_x = -f_{y1.}(VCG - z_{c1}) - f_{y2.}(VCG - z_{c2}) - f_{z1} y_{c1} + f_{z2} y_{c2} \tag{9}$$

where $\vec{f}$ is the resultant force vector, f_{y1}, f_{y2}, f_{z1} and f_{z2} are force components, and m_x is the moment of each section. The total force induced by the roll angle on the sway, roll and yaw motion are approximated by an integration of the section forces along the wetted keel length:

$$f_y = f_{y1} + f_{y2} \quad \rightarrow \quad Y = \int_0^{L_k} f_y \, dx \tag{10}$$

$$K = \int_0^{L_k} m_x \, dx \tag{11}$$

$$N = \int_0^{L_k} x f_y \, dx \tag{12}$$

where Y, K and N are roll-induced forces on the sway, roll and yaw motions, respectively.

CONTACT WITH THE AUTHORS

Kazem Sadati

Hamid Zeraatgar
e-mail: hamidz@aut.ac.ir

Aliasghar Moghaddas

Amirkabir University of Technology
Department of Maritime Engineering
Tehran
Islamic Republic of Iran